

Appendix

The Coupling Coefficient as an Index of Junctional Conductance

Sidney J. Socolar

Department of Physiology and Biophysics, University of Miami School of Medicine,
Miami, Florida 33152

Received 26 October 1976

In the foregoing paper, Azarnia and Loewenstein (1977) suggest that the electrical coupling coefficient in certain strongly coupling cell clones may have been insensitive to demonstrated changes in junctional membrane permeability [*see also* Déléze & Loewenstein (1976)]. In the following, it is shown that the usefulness of the coupling coefficient as a quantitative index of junctional conductance is limited to systems where coupling is relatively weak and where the topology of cell connection is well defined.

The transmittance¹ of membrane channel assemblies linking cells is most often demonstrated in terms of the electrolyte conductance of the cell junction and/or in terms of the diffusion of an injected fluorescent probe molecule. The latter approach lets the investigator characterize the permeance of specific probes chosen for their size or other molecular attributes, or for their possible physiological significance. The electrical approach is less flexible, relying as it does on the particular mix of ions present in the cytoplasm, each species contributing in proportion to the product of its permeability and concentration; on the other hand, it is capable of demonstrating junctional transmittance in cases where even rather small fluorescent molecules appear to be impermeant (*see, for example*, Déléze and Loewenstein (1976) and other references there).

Ultimately, both the junctional conductance and the diffusion permeability—measured optically or otherwise—depend in similar ways on

¹ The term *transmittance* is used here to represent the generic phenomenon of junctional membrane permeability, whether expressed as a conventional membrane permeability or as a membrane conductance.

two properties: the number of channels linking a pair of cells and the effective channel bore as “seen” by the respective permeant². Thus, for example, both the conductance and the diffusion permeability are expected to be proportional to channel abundance and, hence, equally sensitive to a change in abundance, errors of measurement aside. However, for reasons of convenience, in most electrical tests of junctional transmittance what is determined is not the junctional conductance but, rather, the coupling coefficient. To measure this, a cell is driven by an inward or outward current step; the ratio of the steady state values of the transfer voltage, developed across the nonjunctional membrane of a neighboring cell (usually contiguous; voltage hence labelled V_{II}), and the input voltage (V_I), is termed the coupling coefficient. This index is evaluated often without reference to the topology of coupling in the larger cell ensemble of which these cells may be a part. The coupling coefficient is often taken simply as a qualitative index. In any case, it is a direct but nonlinear function of junctional conductance, and the functional relationship between these two quantities, even in a homogeneous cell population, varies with the topology of the coupled cell ensemble. The nonlinearity of that functional relationship can render the coupling coefficient relatively insensitive in a well-coupled system, as compared with the essentially linear optical method, in detecting a change in junctional channel abundance, particularly when the methods are used only qualitatively. This is shown below by examining the functional dependence of the coupling coefficient upon junctional and nonjunctional cell membrane conductances in four different system topologies. These four topologies (Fig. 6) approximate or bracket many one- and two-dimensional cell-group patterns encountered in cultures as well as in some tissues. If g_j is the conductance of a cell junction and g_n the nonjunctional membrane conductance of a cell, the coupling coefficients are always expressible as functions of g_j/g_n and they are most conveniently plotted in that form³ (Fig. 7).

In the derivation of coupling coefficients, the following simplifying

2 This statement overlooks a channel interaction term in the conductance, a term that becomes small when channel diameter is small in relation to interchannel distance. From the best experimental estimate of channel diameter [Simpson, Rose & Loewenstein (1977)] and from structural evidence on the membrane spacing of presumptive channels in the same tissue [Rose (1971)], the cell-to-cell channels of gap junctions would appear to satisfy this condition. [See *also* Revel & Karnovsky (1967), Peracchia & Dulhunty (1976).]

3 This is possible because the coefficient always is a ratio of two resistance expressions, each mathematically a homogeneous function of degree one in g_j^{-1} and g_n^{-1} . Hence we can multiply every term in numerator and denominator by g_j , transforming the coupling coefficient into a function of g_j/g_n .

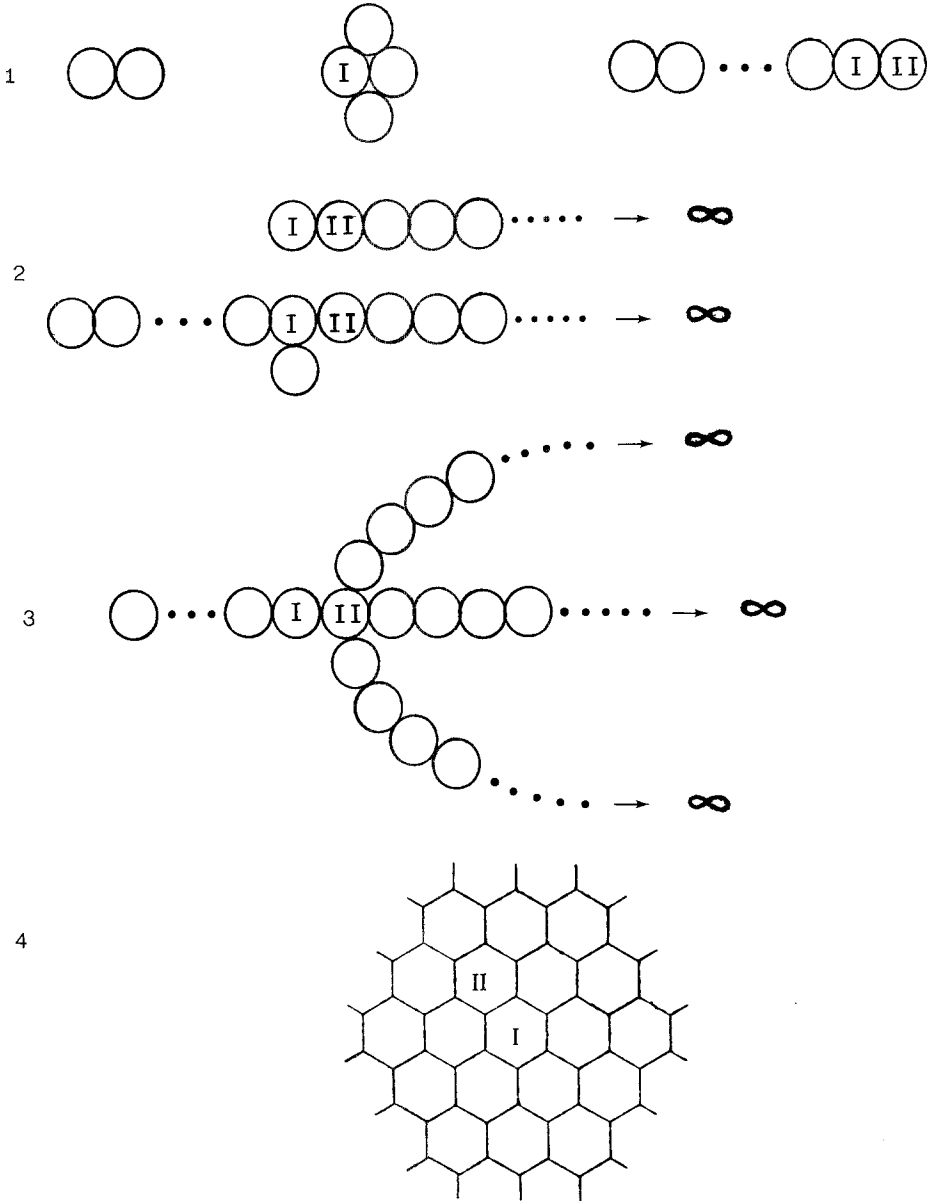


Fig. 6A

Fig. 6(A) Examples of the cell topologies treated. Reference is made to curves in Fig. 7A and B. (1) Three of the alternative configurations corresponding to Eq. (1) and to curves 1. In the center model, cell II is any of the three unlabelled cells. (2) Two of the configurations corresponding to Eq. (2c) and to curves 2. (3) One of the configurations corresponding to Eq. (3c) for the value $m=3$ and to curves 3. (4) Part of the infinitely extended cell monolayer represented by Eq. (4) and by curves 4. (B) Equivalent conductance networks corresponding to the four topologies in A. Nonjunctional conductances are left unspecified on the cell I side of each I:II junction. In 4, each internodal conductance element is g_j ; each node-to-ground element, g_n

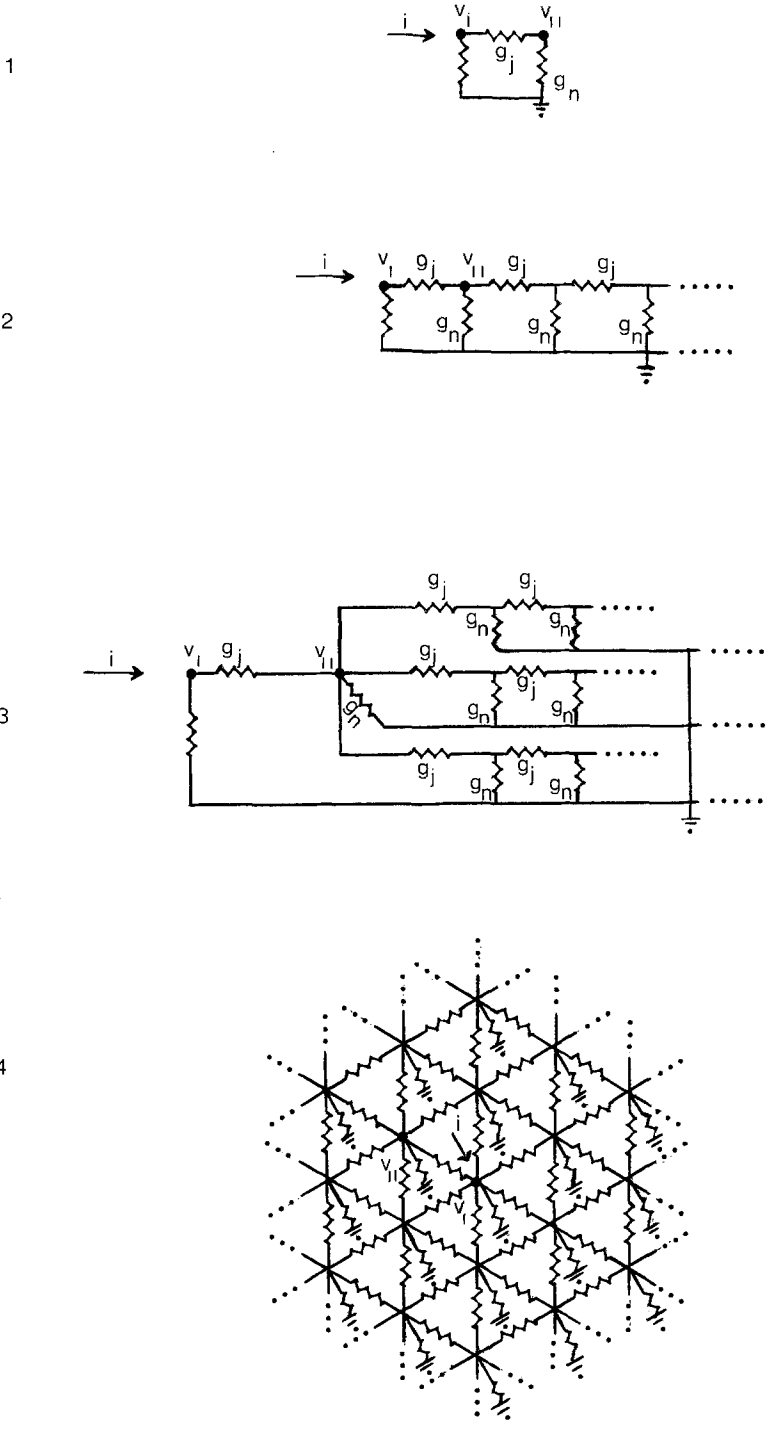


Fig. 6B

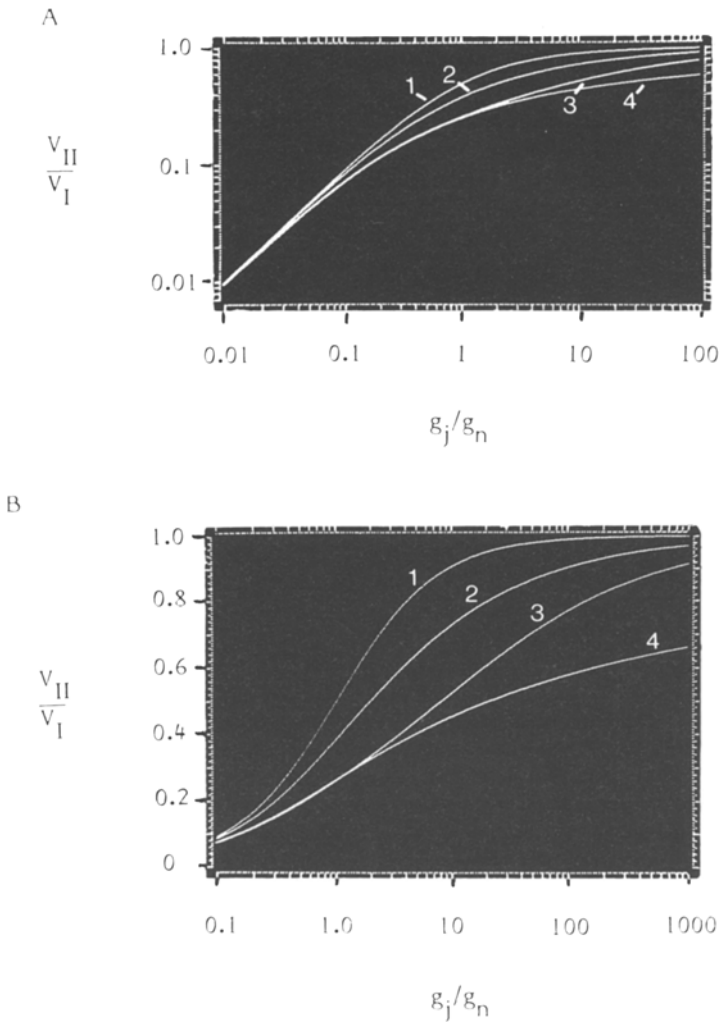


Fig. 7. Coupling coefficient (V_{II}/V_I) as a function of the ratio of junctional and non-junctional cell membrane conductances (g_j/g_n). Curves 1, 2, 3, and 4 represent corresponding topologies in Fig. 6. Coupling coefficient is plotted on logarithmic ordinate in A, on linear ordinate in B; note incomplete overlap of abscissa ranges in A and B

assumptions are made: (1) all cells of a coupled system have identical values of g_j and g_n , respectively⁴; (2) perijunctional insulation conductance (Loewenstein, Nakas & Socolar, 1967) is negligibly small in 4 A less restrictive assumption suffices. As already indicated, the driven cell is taken by convention to be cell I, to which cell II is contiguous. Once these cells have been identified, they specify the coupling coefficient in a form that is independent of the conductance parameters of any cells coupled to I and II from side I only. In view of this, in the Fig. 6B equivalent networks, nonjunctional conductances on the cell I side of I:II junctions, have been left unspecified.

comparison with g_j and g_n ; (3) the interior of each cell is isopotential; (4) the extracellular medium is isopotential.

Topology 1: Cell II is Terminal.

The defining property of this topological class is that no cell is coupled to cell I via cell II unless also coupled directly to cell I (Fig. 6A.1 and B.1). The simplest system of the class is the coupled cell pair. For all systems of this class the coupling coefficient is given by

$$\frac{V_{II}}{V_I} = \frac{g_j/g_n}{1 + g_j/g_n}. \quad (1)$$

See Fig. 7A and B, curves 1.

Topology 2: Cell II Is Followed by and Coupled to an Infinitely Long Linear Chain of Cells

The ratio of the “length constant” of a linear coupled system to the cell length is $\sqrt{g_j/g_n}$. When and only when this ratio is sizeable, junctional resistance may be treated as if continuously distributed along the length of the system⁵; and the resulting value of the coupling coefficient in this infinite linear cable approximation is $\exp(-\sqrt{g_n/g_j})$. To derive an expression that remains valid at low values of space constant, I use a lumped resistance model (Fig. 6A.2 and B.2). For purposes of the derivation, cell I is conveniently taken to be the initial cell of the chain. (It can readily be shown that the coupling coefficient thus derived is valid even when cell I is not initial, as in the second case in Fig. 6A.2.) Let i represent the amplitude of a step current injected into cell I ; V_I , the corresponding steady state potential shift in that cell; and V_{II} , that in cell II . Define $g_{in} = i/V_I$. Then

$$g_{in} = g_n + \frac{g_j g_{in}}{g_j + g_{in}}, \quad (2a)$$

since, because the chain has an infinite number of cells, g_{in} , the input conductance seen from cell I , is equal to the input conductance that would be seen from cell II if cell I were absent. The coupling coefficient is

$$\frac{V_{II}}{V_I} = \frac{g_j}{g_j + g_{in}}. \quad (2b)$$

⁵ Interpreting the measured coupling coefficient in terms of the continuous model would lead to a $2\times$ underestimation of g_j/g_n when its true value is 0.1, and to a $200\times$ underestimation when it is 0.01.

From Eqs. (2a) and (2b), it follows that

$$\frac{V_{II}}{V_I} = \frac{g_j/g_n}{1/2 + g_j/g_n + \sqrt{1/4 + g_j/g_n}}. \quad (2c)$$

Eq. (2c) is plotted as curves 2 in Fig. 7A and B.

Topology 3: Cell II is Followed by and Coupled Directly to m Parallel, Infinitely Long Linear Chains of Cells.

Here, as in the preceding section, a lumped resistance model is used. Again, the starting assumption will be made that cell I is coupled to cells other than cell II only via cell II, but again the validity of the derived coupling coefficient will not be restricted to this condition (Fig. 6A.3 and B.3).

Now we have

$$\frac{V_{II}}{V_I} = \frac{g_j}{g_j + g_n + \frac{m}{1/g_j + 1/g_f}}, \quad (3a)$$

where, by analogy with Eq. (2a),

$$g_f = g_n + \frac{g_j g_f}{g_j + g_f}. \quad (3b)$$

From (3a) and (3b),

$$\frac{V_{II}}{V_I} = \frac{g_j/g_n}{1 + g_j/g_n + m(\sqrt{1/4 + g_j/g_n} - 1/2)}. \quad (3c)$$

Now Eq. (2c) can be seen as a special case of (3c) for the condition $m=1$. In Fig. 7A and B, curves 3 represent Eq. (3c) for $m=3$.

Topology 4: Infinitely Extended Monolayer;

Each Cell has Six Nearest Neighbors, to Which It is Coupled Directly.

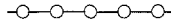
This is the topology (Fig. 6A.4 and B.4) whose coupling pattern has been characterized by Siegenbeek van Heukelom, Denier van der Gon & Prop (1972):

$$\frac{V_{II}}{V_I} = k^{-1} \left[1 - \frac{E(k^2)}{K(k^2)} \right], \quad (4)$$

where

$$k = 1 + \frac{g_n}{4g_j} - \left[\left(\frac{g_n}{4g_j} \right)^2 + \frac{g_n}{2g_j} \right]^{1/2},$$

$K(k^2)$ is the complete elliptic integral of the first kind, and $E(k^2)$ is the complete elliptic integral of the second kind. In Fig. 7, Eq. (4) is plotted as curves 4.



Topology-related variations in the coupling coefficient can all be understood qualitatively in terms of the two-cell case and the variations imposed on Eq. (1). Changes in coupling pattern can be interpreted as introducing shunts across one or more of the three conductances in the two-cell model. To the extent that g_n of cell *II* is shunted proportionately more than g_j , the coefficient is reduced in value. If, as in the center case in Fig. 6 *A.I*, the shunts are in equal proportion, the coefficient retains the same value it would have for a cell pair.

Figure 7 makes clear that at high values of junctional conductance (relative to nonjunctional conductance) the coupling coefficient is rather insensitive to junctional conductance changes. Thus, if a cell pair displaying a coupling coefficient of 0.8 is compared with a pair in which junctional channel abundance is reduced tenfold, the coupling coefficient measured in the latter is smaller by less than threefold. In the other topologies shown, a similar reduction in channel abundance causes less than a twofold drop in the value of the coupling coefficient. If, on the other hand, the starting point for comparisons is a coupling coefficient equal to 0.1, a tenfold diminution of channel abundance shows up as a seven-to-ninefold drop in the size of the coupling coefficient, nearly a proportional response. Thus, only in weakly coupled systems is the coupling coefficient as sensitive a function of junctional transmittance as is transjunctional diffusion rate.

Furthermore, Fig. 7 brings out another limitation of the coupling coefficient as an index of junctional transmittance—its strong dependence on the topology of interconnection especially in a well-coupled cell ensemble. For example, in relation to the topologies represented in Fig. 7 *B*, a measured coupling coefficient of 0.6 may reflect a junctional-/nonjunctional conductance ratio falling anywhere in a range of two orders of magnitude.

In representing the coupling coefficient as a function of g_j/g_n , the equations and graphs emphasize that the coefficient is equally sensitive to changes in junctional or nonjunctional conductance.

I thank Messrs. Jim Gray and John Stolfi for their help in making the computer-generated graphs.

References

- Azarnia, R., Loewenstein, W.R. 1977. Intercellular communication and tissue growth. VIII. A genetic analysis of junctional communication and cancerous growth. *J. Membrane Biol.* **34**:1
- Déléze, J., Loewenstein, W.R. 1976. Permeability of a cell junction during intracellular injection of divalent cations. *J. Membrane Biol.* **28**:71
- Loewenstein, W.R., Nakas, M., Socolar, S.J. 1967. Junctional membrane uncoupling. Permeability transformations at a cell membrane junction. *J. Gen. Physiol.* **53**:498
- Peracchia, C., Dulhunty, A.F. 1976. Low resistance junctions in crayfish. Structural changes with functional uncoupling. *J. Cell Biol.* **70**:419.
- Revel, J.P., Karnovsky, M.J. 1967. Hexagonal array of subunits in intercellular junctions of the mouse heart and liver. *J. Cell Biol.* **33**:C7
- Rose, B. 1971. Intercellular communication and some structural aspects of membrane junctions in a simple cell system. *J. Membrane Biol.* **5**:1.
- Siegenbeek van Heukelom, J., Denier van der Gon, J.J., Prop, F.J.A. 1972. Model approaches for evaluation of cell coupling in monolayers. *J. Membrane Biol.* **7**:88
- Simpson, I., Rose, B., Loewenstein, W.R. 1977. Size limit of molecules permeating the junctional membrane channels. *Science* **195**:294.